BED-Vol. 50, 2001 Bioengineering Conference
ASME 2001

PULSATILE BLOOD FLOW IN A TAPERED FEMORAL ARTERY OF A DOG: MEASUREMENTS AND COMPUTED HEMODYNAMICS

Rupak K. Banerjee (1), Lloyd H. Back (2), Young I. Cho (3)

(1) Department of Mechanical Engineering
Kettering University
Flint, MI

(2) Jet Propulsion Laboratory
California Institute of Technology
Pasadena, CA

(3) Mechanical Engineering and
Mechanics Department
Drexel University
Philadelphia, PA

INTRODUCTION

This investigation presents *in-vivo* measurements of flow quantities and numerical flow and pressure computation and validation, using measured flow parameters, vessel dimensions and blood viscosity, in a mildly tapered femoral artery of a living dog. While such a combined experimental-calculation approach may appear straightforward in principle, there are concerns about the reliability of *in vivo* measurements, and the appropriateness of the method of flow computation with regard to the non-Newtonian viscosity of blood, wall and inlet boundary conditions, and handling of the nonlinear convective acceleration terms and coupling of the pressure and velocity fields during the cardiac cycle.

In the flow computations, blood viscosity was assumed to be dependent upon shear rate, which, in turn, results in relatively unimportant elastic and time relaxation effects. This is believed to be a reasonable approximation for blood flow through arteries of the size of the femoral in a dog. Since the arterial wall in general is very complex, being anisotropic (elastin, collagen, smooth muscle), viscoelastic (creep, stress relaxation, hysteresis), and under a mean and fluctuating state of three-dimensional stresses, it is very difficult to specify its dynamic behavior with certainty in computational methods. Hence, the computations are for a rigid wall and an elastic wall.

METHODS

A tracing of the X-ray of a portion of the femoral artery of a dog where the measurements were made previously at USC School of Medicine is shown in Fig. 1. The pressure drop across the segment is measured by using two small branch arteries, which are ligated and connected by tubing to a Validyne transducer. The cuff for the Doppler flow meter is located near the first branch as shown in Fig. 1. The vessel segment (Fig. 1) is simplified and kept to be relatively straight with mild taper. The vessel diameter at the first branch tap is d_1 = 3.8 mm, and at the second branch tap is d_2 = 3.6 mm. The axial distance between the branch pressure taps is 52 mm.

The flow simulations were carried out by solving the mass and momentum equations for pulsatile laminar blood flow using a Galarkin Finite Element Method (FEM) [1]. The Carreau model was used for shear rate dependent viscosity of blood with local shear rate calculated from the velocity gradient through the second invariant of the rate of strain tensor [2]. Details of the finite element method for a rigid wall were given by Banerjee et al. [3].

The mathematical modeling of compliant wall problems, which needs Fluid Structure Interaction (FSI) capabilities [4], requires the concurrent application of techniques from Computational Fluid Dynamics (CFD), Computational Solid Dynamics (CSD) and Computational Mesh Dynamics (CMD) fields. In the solution strategy adopted, all the three steps are performed sequentially.

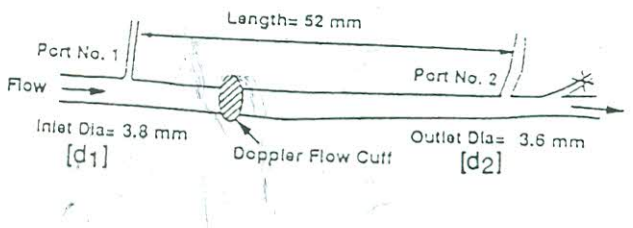

Fig. 1 X-ray tracing of portion of the femoral artery of a living dog. Ligated small branch arteries are marked port No. 1 and 2.

The CFD step consists of the solution of the flow problem on a given mesh. The exchange of information with the CSD and CMD problem happens at the fluid-structure interface. As a part of the flow solution, the traction on the interface nodes are computed, which are used as loads for the CMD. In transient problems, the velocities at the interface are computed as part of the CSD step and applied as

boundary conditions for the Navier Stokes equation of CFD. The exchange of information with the CMD step is done via the repositioning of the nodes of the fluid domain, after each update of the configuration of the structure. Details are given in the conference.

RESULTS AND DISCUSSION

Computations were carried out consistent with the calibrated Doppler flow meter. The flow signal was tri-phasic with a brief period of reverse flow during the early part of diastole. Using a digital voltmeter, the time-averaged blood flow velocity, u_a = 15.1 cm/sec, and the time averaged pressure drop Δp_a = -0.59 mmHg were obtained. The resting heart rate was 128 beats/min, the period T of a heart beat was 0.47 sec. Measurement of the viscosity of the dog's blood at *in-vivo* temperature gives η =0.037 poise, and the measured blood density, ρ, was 1.04 gm/cm^3.

The time-averaged flow rate Q_a ($=u_a A_1$) based on the upstream vessel diameter d_1 (3.8 mm) was 102 ml/min. Since the mean flow Reynolds number Re_a ($=4Q_a/\pi\, \nu d_1$) was 161, the flow is expected to be laminar. Considering the mean diameter ($\bar{d}$ = 3.7 mm) the time-averaged value of the pressure drop Δp_a using the Poiseuille relation, $\Delta p_a = -[128\eta l\, Q_a]/[\pi\, \bar{d}^{\,4}]$ is –0.54 mmHg. A further correction for mildly uniform taper can be made from the momentum consideration; this then gives a value of Δp_a = -0.57 mmHg. Since the measured value of Δp_a is only about 3% higher, this affords a reasonable estimate of the mean pressure drop and gives confidence in the accuracy of the measurement technique. Also the time-averaged value of the wall shear stress $(\tau_w)_a$ using the Poiseuille relation, $[(\tau_w)_a = (32\eta Q_a)/\pi \bar{d}^{\,3}]$, is 12.7 dynes/cm^2. The dimensionless frequency parameter, $[\alpha = 0.5 d_1 \sqrt{\omega/\nu}\,]$ is 3.7.

The results of the rigid wall computations of $\Delta p(t)$ are shown in Fig. 2A; Fig. 2B (below) is the measured inlet core velocity u_{cl}. The calculated pressure drop has a maximum value of –6.7 mmHg at t = 0.087 s (represented by the upward spike) during peak systole and reaches 3.1 mmHg at t = 0.192 s during early diastole (represented by the downward spike). Experimentally measured peak pressure are –4.5 mmHg at t = 0.110 s during systole and 2.7 mm of Hg at t = 0.225 s during the early diastolic phase of flow. For mid diastole, the second peak pressure drop is also over estimated (-3.0 compared to -1.7 mmHg) and in late diastole, a pressure rise was calculated, but a pressure drop was measured. Numerical calculation of the average pressure drop is –0.645 mmHg, whereas the experimental data show a value of –0.59 mmHg. The 10% difference between the calculated and measured average pressure drops shown in Fig. 2A by the horizontal lines, is relatively small compared to the Δp oscillations during the cardiac cycle.

During the acceleration part of the flow the predicted peak pressure drop $-\Delta p_p$ is obtained at t = 0.087 s (Fig. 2A). From Fig. 2B, a peak Doppler velocity $u_{c\text{-}p}$ is obtained at t = 0.12 s. This indicates a phase-lag between predicted (Δp_p) and measured $u_{c\text{-}p}$ that amounts to θ =-25 deg., since $u_{c\text{-}p}$ lags predicted ($-\Delta p_p$). At the beginning of diastole, flow reversal occurred u_{cl} = -7.7 cm/s at t = 0.24 s. While the peak in the predicted adverse pressure gradient $+\Delta p_p$ occurred at an earlier time so that the phase angle was –37 deg. For the second smaller peak flow $u_{c\text{-}p}$ at t=0.33 s, the phase angle was about –27 deg. These calculated phase angles are within the range of 0 to –60 deg., known for physiological flows, and indicated a hysteresis effect between predicted (Δp) peaks and measured u_c. The predicted (Δp) peaks appear to precede the measured (Δp) peaks by phase angles of –18 to –46 deg., progressively increasing during the cardiac cycle.

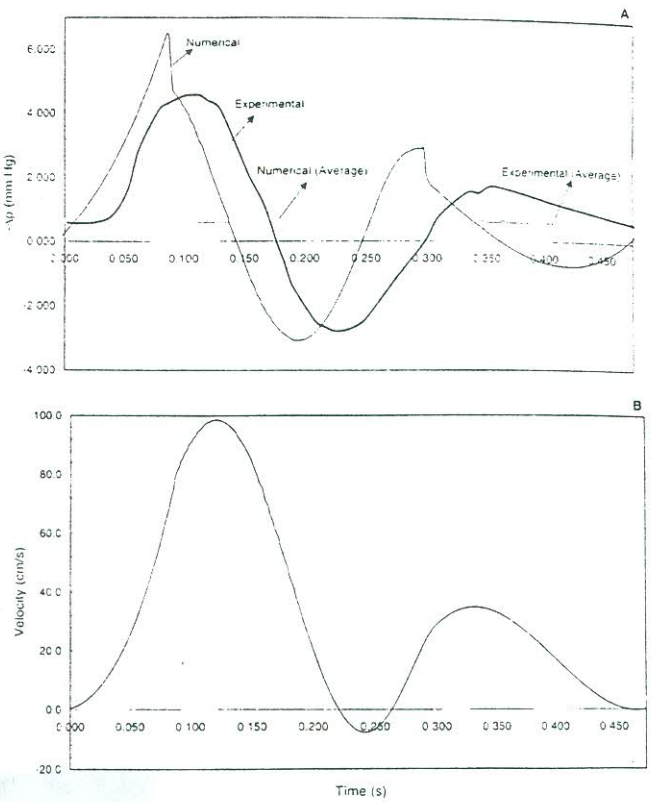

Fig. 2 Temporal variation of pressure drop at wall between port No. 1 and port No. 2 along a pulse cycle (Fig. 2A) for rigid wall. Fig. 2B is the measured inlet core velocity u_{cl}.

The results of the coupled hemodynamic-elastic wall computations will be reported at the conference in conjunction with the measured arterial pressure $p_a(t)$ in the iliac artery bifurcation with a catheter.

REFERENCES

1. Baker, A.J., 1983, *Finite Element Computational Fluid Mechanics*, Hemisphere Publ. Co., Chap. 4, pp. 153-230
2. Banerjee, R.K., Back, L.H., Back, M.R., and Cho, Y.L., 1999, "Catheter Obstruction Effect on Pulsatile Flow Rate – Pressure Drop During Coronary Angioplasty" ASME J. of Biomech. Engrg, Vol. 121, pp. 281-289.
3. Cho, Y.I., and Kensey, K.R., 1991, "Effects of the non-Newtonian Viscosity of Blood on Flows in a Diseased Arterial Vessel: Part 1, Steady Flows," Biorheology. Vol. 28. pp. 241-262.
4. FIDAP Manual, 2000, Fluent Incorporated, Lebanon, NH.